EarlyView publication on wileyonlinelibrary.com
(issue and page numbers not yet assigned;
citable using Digital Object Identifier – **DOI**)

Phys. Status Solidi A, 1–6 (2011) / **DOI** 10.1002/pssa.201026729

Structural and magnetic phenomena in ultrathin C/Co/C stacks prepared by DC magnetron sputtering

A. Zolotaryov[*,1], Ye. Bugayev[2], V. Samofalov[1], O. Devizenko[1], E. Zubarev[1], S. Martens[2], O. Albrecht[3,2], D. Görlitz[2], and K. Nielsch[2]

[1] Metal and Semiconductor Physics Department, "Kharkiv Polytechnic Institute", National Technical University, 21 Frunze st., 61002 Kharkiv, Ukraine
[2] Institut für Angewandte Physik, Universität Hamburg, Jungiusstr, 11, 20355 Hamburg, Germany
[3] Institut für Mikrosystemtechnik (IMTEK), Universität Freiburg, Georges-Koehler-Allee 103, 79110 Freiburg, Germany

Received 30 November 2010, revised 27 January 2011, accepted 1 February 2011
Published online 28 February 2011

Keywords cobalt, magnetic anisotropy, magnetic properties, sputtering, structure, thin films

[*] Corresponding author: e-mail azolotar@physnet.uni-hamburg.de, Phone: +49 (0)40 42838 5248, Fax: +49-(0)40-42838-3589

We study two C(5 nm)/Co/C(5 nm) multilayer stacks with cobalt layer thicknesses of 4 and 13 nm. Structural analysis of fabricated systems reveals corresponding cobalt layers to be in amorphous (nanocrystalline) and [0001]-textured *hcp*-phase. The magnetic measurements for both systems agree well with structural data. For the amorphous cobalt layer magnetic data reveal the absence of carbides, high saturation field of 1.6×10^4 Oe and vanishing inplane coercive field. We also show that strong inplane anisotropy can be introduced into the amorphous cobalt film by controlling the process parameters of DC-magnetron sputtering. For the textured *hcp*-cobalt film we have deduced the presence of randomly close-packed (*rcp*) structure. We assume this defect-rich cobalt *hcp*-phase to be responsible for the detected elimination of the out-of-plane magnetic anisotropy in the corresponding multilayer sample.

1 Introduction Within the last two decades thin film multilayer systems have enjoyed much attention due to the continuously increasing amount of novel applications they can enable. The unique optical [1, 2], magnetoelectric [3] and magnetic [4] properties have recently determined the major research directions for artificial multilayer thin-film systems. Metallic ferromagnetic cobalt films embedded between the conducting nonmagnetic carbon layers can be of potential interest for the above-mentioned applications [5–7].

The cobalt-based alloys can also be used for magnetic data storage media and read/write heads. The storage systems of the near future show the trends of 1 Tb per square inch for data density and of 2 Gb per second for data writing speed and even more [8]. Both trends require the development of new magnetic materials with preassigned properties. Storage media require films of high coercivity having magnetically decoupled nanoscale particles. Head fabrication calls for materials with vanishing coercive field ($H_c < 1$ Oe) and high saturation field ($B_S = 2 \times 10^4$ Oe).

Recent reports predict that the expected magnetic properties of ferromagnetic multilayer Co/C systems can be reached after the extreme downscaling of their dimensions (*z*-dimension along the film surface normal or the granule size) [9–11]. During this downscaling an amorphization of cobalt phase takes place that decreases the film saturation magnetization and simultaneously destroys the inplane coercive field [9, 10]. Furthermore, the simultaneous increase of the role of surface intermixing in ultrathin Co/C films leads to formation of complex nonmagnetic compounds [12, 13]. Both phenomena exhibit presumably a negative influence on the overall magnetic properties up to their total loss [9, 10]. The control over these effects as well as their elimination or suppression within the film-preparation process has become a main goal for the experimentalists in the field.

The insight into the structural and magnetic properties of ultrathin C/Co/C film systems prepared by DC-magnetron sputtering process is presented in this work. Combination of

structural and magnetic analysis provided us with detailed description of the internal structural transformations defining the unique magnetic properties of the investigated systems.

2 Tools and methods Structure analysis was done using a transmission electron microscopy (TEM) with acceleration voltage of 100 keV and a lab X-ray diffractometer equipped with the Cu anode and primary asymmetrically cut Si (110) monochromator ($CuK\alpha_1$ radiation) for small-angle X-ray reflectometry (XRR) or secondary graphite (0001) monochromator for X-ray phase (XRD) analysis.

The static magnetic properties were investigated using superconducting quantum interference (SQUID), vibrating-sample (VSM) and magneto-optical Kerr (MOKE) magnetometers [14].

A MPMS XL^{TM} SQUID ($H_{max} = 50$ kOe, resolution 10^{-6}–10^{-5} emu) was applied to measure hysteresis loops of the cobalt films positioned with the film surface perpendicular (out-of-plane setup) to the applied magnetic field. The measurements were done at 10 K sample temperature. The initial signal intensities of the magnetization curves were measured in (emu) units and for out-of-plane data output were additionally normalized to the volume of constituent cobalt layers. The SQUID measurements of our samples enable high measurement precision in the fields starting from 50 Oe.

Angular-dependent hysteresis loops of the investigated samples were measured in the longitudinal inplane setup (film surface parallel to the external magnetic field vector) with a NanoMOKE-2^{TM} magnetometer. These measurements were done at room temperature (RT) using the applied magnetic fields up to 800 Oe. The data obtained from the MOKE measurements are initially normalized to the maximum magnetization values.

For the high-resolution analysis of hysteresis loops in low fields (<50 Oe) we also used the commercial cryocooler-based VSM of VersaLab. The measurements were done in the inplane setup at RT. The experimental resolution was better than 10^{-6} emu.

3 Sample preparation The C/Co/C thin-film stacks were prepared using DC magnetron sputtering of carbon (purity 99.99%) and cobalt (99.95%) targets in argon atmosphere with working pressure 0.17 Pa. The base pressure in the argon-free chamber before sputtering process was 0.1 mPa. Commercial silicon substrate pieces ($5 \times 5 \times 0.5$ mm^3) were used. For TEM analyses float glass was used as a substrate and gelatin was applied to separate the deposited C/Co/C system. The stack deposition was enabled in two different runs (see Fig. 1):

(i) By stepwise substrate movement over the targets with 50 Oe radial component of the magnetron magnet.
(ii) By single-substrate exposure over the center of each target (position A in Fig. 1) with vanishing radial component of magnetron magnetic field and then rapid movement to the other target.

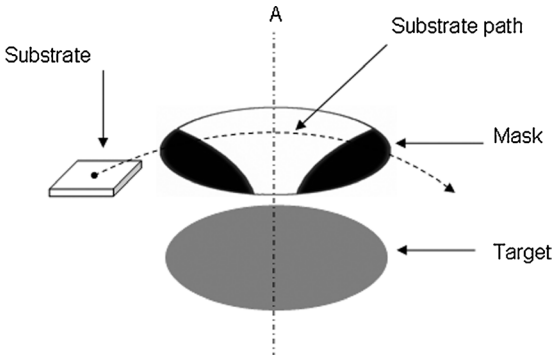

Figure 1 Visualization of different sample-exposure modes during the DC-sputtering process. In one case, the sample is stepwise moved over the magnetron target (substrate pass curve), in another case the sample is rapidly moved to the target center (position A) and after the exposure time rapidly moved outside of the target. The front side of the rectangular sample moving along the substrate pass line is defined as "label"-side. This labeling is used for the sample alignment for VSM measurements, see Fig. 6.

Run (a) was used for fabrication of samples A and B, and run (b) was applied for fabrication of a twin sample to sample A (see below). The deposition rates were 0.1 nm/s for carbon and 0.3 nm/s for cobalt. Substrate temperature during deposition was lower than 323 K.

From our previous results we know that in the Co/C multilayer system with Co thickness varying in the nm-scale structural transformation of cobalt layer takes place [15, 16]. The effect is visualized in Fig. 2 where a plan-view TEM image of the C/Co/C film with cobalt thickness gradient of 0.04 nm/mm (left to right) is shown. It can be seen that the

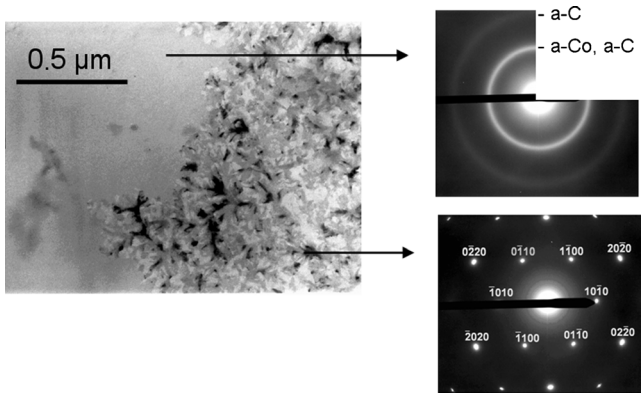

Figure 2 TEM micrograph (plane bright-field view) of the C/Co/C stack with gradient thickness of the cobalt layer (the whole image area represents transformations within the $t_{Co} = 5.8$ nm). Both shown selected-area electron diffraction patterns demonstrate the film structure at the opposite sides of the Co crystallization front. On the left side of the image the film material is a distorted amorphous phase, on the right side metal layer is a single-crystal-like phase of *hcp* Co with [0001] zone axis parallel to the film surface normal.

cobalt film with thickness $t \leq 5.8$ nm is in an amorphous state. Above $t_{Co} = 5.8$ nm explosive crystallization occurs in the cobalt film. This leads to the formation of quasi-single-crystalline (strongly textured polycrystalline) *hcp*-cobalt phase with average grain size of 0.2–0.3 μm and [0001]-zone axis parallel to the film surface normal. This structural transformation takes place already during the cobalt film growth. This was confirmed with *in situ* electric conductance measurements.

Taking into account the structural transformation of cobalt film described above, for our current study we have grown two main three-layer stacks (Fig. 3) with thickness of carbon films of 5 nm each and the nominal thicknesses of cobalt films of 4 nm (sample A) and 13 nm (sample B), respectively, possessing cobalt film thicknesses below and above the critical value for explosive crystallization. The carbon layer thickness 5 nm is enough to protect the Co layer from the substrate and the ambient air influence [17]. In addition, a three-layer stack is a model unit for the Co/C multilayer system that has been developed for the reflective coating in X-ray microscopy of a "carbon window" ($\lambda \sim 4.5$ nm) [2, 18].

The final stack properties (constituent layer thickness, interface widths, and layer densities) were monitored by XRR. This revealed corresponding layer thicknesses close to the nominal values (with estimation uncertainty of 1%) and low interfacial roughness (~0.5 nm).

4 Results and discussion Symmetric θ–2θ XRD data for samples A and B are shown in Fig. 4. Consistent with our expectations, these data prove that cobalt films in samples A and B are correspondingly in amorphous and *hcp* single-crystal-like ([0001]-textured) states. Plan-view TEM data for both samples support the XRD result.

It is known that in the case of close-packed systems extinguishing of diffraction peaks from the condition h–$k = 3n \pm 1$, $l \neq 0$, where n is an integer, h, k, l are Miller indices, directly points on the random close packed (*rcp*) structure [19]. The X-ray curves for sample B measured in the asymmetric scan geometry (offset Ω was set up to detect reflection from (103) planes) exhibited vanishing of the corresponding peaks. Taking into account the TEM and symmetric XRD data for crystalline cobalt film (Fig. 2 and Fig. 4) the *rcp* ordering in the *hcp*-cobalt can be associated with stacking faults (locally formed fcc-substructures) within the *hcp*-phase.

The results of MOKE measurements on samples A and B are shown in Fig. 5. The following characteristic features can be detected here. First off all, both samples are

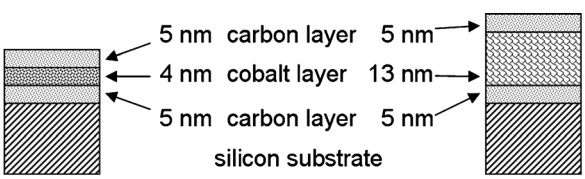

Figure 3 Scheme for sample A (left) and sample B (right).

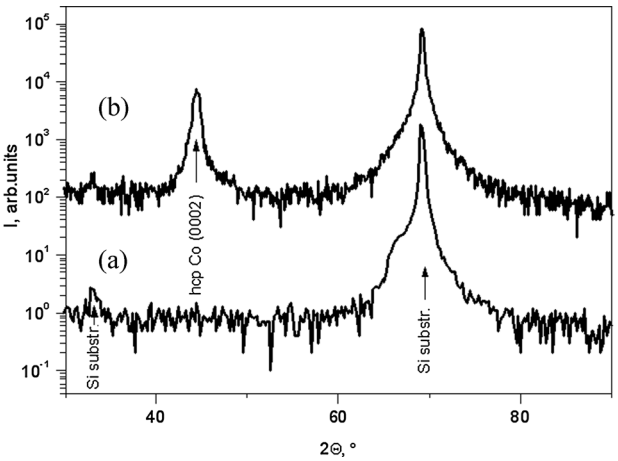

Figure 4 X-ray diffraction profiles for the C/Co/C multilayer stacks A (a) and B (b) with correspondingly amorphous and *hcp*-cobalt phases. An absence of peaks except for the Co(0002) reveals the [0001] textured structure.

ferromagnetic. Secondly, a magnetization reversal process for the samples A and B in both cases led to the hysteresis loops with high squareness factor. This can be related to the "thin-film" magnetic nature of 4-nm and 13-nm thick cobalt layers where the easy magnetization axis (main component of magnetization vector) lays in the plane of the thin film. Thirdly, the coercive fields for sample A (≈3 Oe) and sample B (≈40 Oe) differ from each other by a factor of more than 10. This indirectly confirms the difference in crystalline states of the corresponding samples.

In addition, the data in Fig. 5 reveal the presence of noticeable induced single-axis in-plane anisotropy in sample A with amorphous cobalt. We relate this effect to the stepwise substrate movement in the external magnetic field parallel to the film surface during the DC-sputtering process [20, 21]. As a proof, we applied the sputtering in the different runs (sputtering on the moving or stationary sample) as it is described in Section 3. Both experiments led either to formation of the cobalt layer with the uniaxial in-plane anisotropy (Fig. 6i) or isotropic in-plane magnetic structure (Fig. 6(ii)). For sample B, such in-plane anisotropy is difficult to resolve due to the high coercive force (40 Oe). Complementary measurements using the magnetic precipitates (bitter pattern technique) have also approved the presence of the induced in-plane magnetic anisotropy also in sample B. From these results it can be concluded that the thin-film C/Co/C system provides a high sensitivity to the external magnetic field variations during the DC-magnetron sputtering process independent of the crystalline state of cobalt layer.

Hysteresis loops of samples A and B measured using a SQUID magnetometer in the out-of-plane setup are presented in Fig. 7. Experimentally estimated H_S for the sample A is not less than 16 ± 1 kOe. In the thin-film magnetic system the saturation field along the hard magnetization axis (perpendicular to thin film surface) is $H_S \approx 4\pi M_S - H_K$,

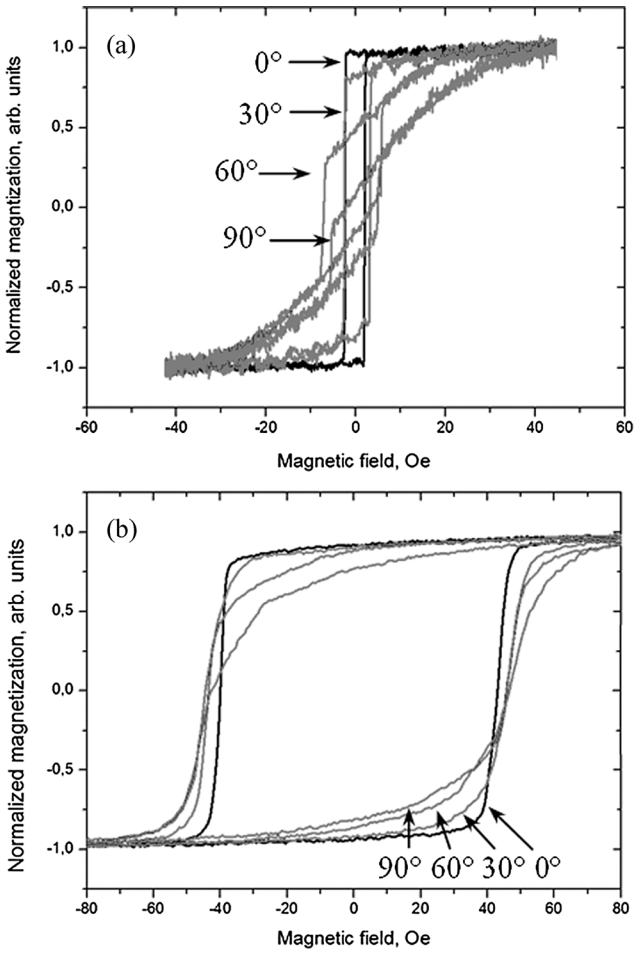

Figure 5 Angular-dependent MOKE measurements of sample A (a) and sample B (b). The shown curves correspond to orthogonal angular sample positions (0 and 90°) and the intermediate angular states (30 and 60°). During 360°-MOKE measurements the 0 and 90° loops repeat with 180°-symmetry defining the uniaxial in-plane anisotropy axis. For sample A the uniaxial anisotropy is more distinct in comparison to sample B.

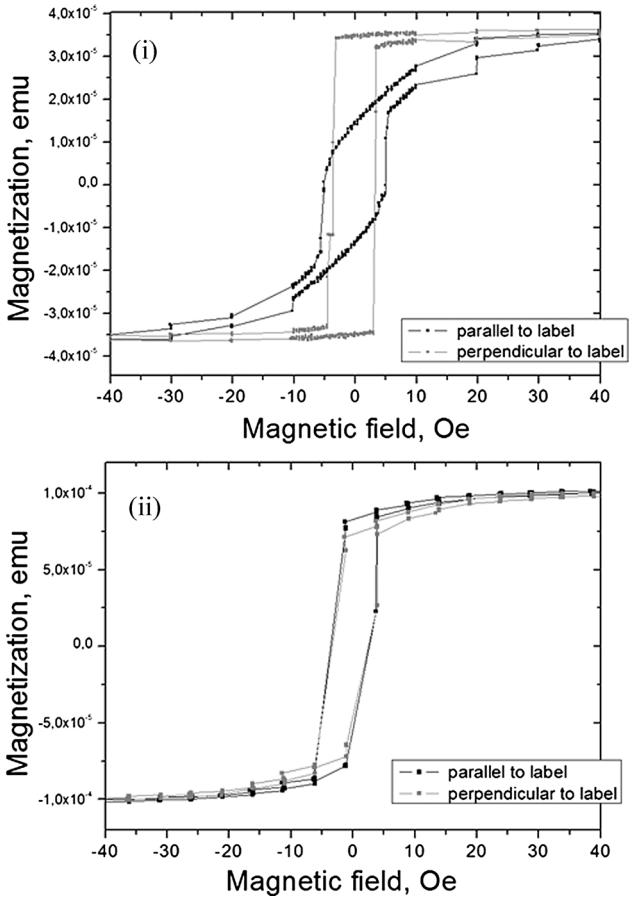

Figure 6 The in-plane VSM data for samples A (i) and twin sample (ii) correspondingly deposited in runs (a) or (b) (see Section 3) and measured along the labeled direction and along the orthogonal direction (see Fig. 1 caption). Nonequivalence in hysteresis loops (i) and their total coincidence (ii) reveals that strong induced anisotropy is a result of substrate transport in an external magnetic field (50 Oe) of the magnetron source.

where M_S is the saturation magnetization value and H_K is the natural uniaxial anisotropy field with the easy magnetization axis oriented parallel to the film surface normal. In the case of amorphous thin Co film, H_K is expected to vanish ($H_K \ll 4\pi M_S$) and $H_S \approx 4\pi M_S$. Based on this approach the M_S value for sample A estimated from the experimental saturation field H_S is 1200 ± 100 emu/cm^3. The M_S value directly extracted from the experimental curve reveals a comparable result of 1150 ± 100 emu/cm^3. This not only supports the expected absence of the out-of-plane uniaxial anisotropy in the sample A but also directly reveals the amorphous nature of the involved cobalt film.

The amorphization with vanishing thickness of pure cobalt film in the C/Co/C system we previously tentatively associated with an increasing role of interfacial intermixing effects (which we already observed in other multilayer systems [22]) whereby formation of amorphous Co_2C

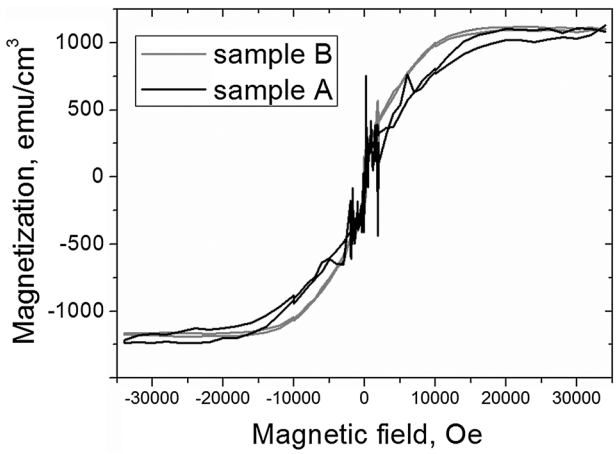

Figure 7 SQUID measurements of samples A and B in the out-of-plane setup.

Table 1 Comparison of structural and magnetic data of our samples A and B with literature results for sputtered Co/C thin-film systems. Label "X" points to the absence of ferromagnetic signal. Label "-" notes that the data were not explicitly mentioned in the original paper.

system	cobalt phase	t, (nm)	M_S, (emu/cm^3)	in-plane H_c, (Oe)	reference
C/Co/C (sample A)	a-Co + C (carbide free)	4	1150 ± 100	3–5	results from this study
$Co_{(0.6)}C_{(0.4)}$	a-Co + C (carbide)	5–100	X	X	[9]
Co/C	a-Co + C (carbide)	3	X	X	[10]
Co/C	a-Co + *hcp*-Co	4	570	5	[10]
$(Co/C)_n$ sputtering in $Ar/H_2/CH_4$	am./nanocryst.	40	1050	1.6	[11]
C/Co/C	*hcp*-Co	14	–	80	[12]
$Co_{(0.66)}C_{(0.33)}$	δ-Co_2C (carbide) + *hcp*-Co	20	285	–	[26]
C/Co/C (sample B)	*hcp*-Co	13	1200	50	results from this study

carbide was indirectly assumed [23]. Up to now, the amorphous nature of such an ultrathin C/Co/C stack did not allow us to use structure analysis tools to prove or disprove this assumption. The magnetic data in Fig. 7 clearly answer this question: taking into account nearly equal volume-normalized M_S values determined from the experimental magnetization and saturation fields for samples A and B (pure *hcp*-cobalt), we conclude that there are no nonmagnetic phases (e.g., cobalt carbides [24]) in the assumed amorphous Co:C compound of sample A.

The experimental H_S value for sample B extracted from Fig. 7 is 18–18.5 kOe. This saturation field lies close to the well-known tabulated value for the bulk cobalt phase ($4\pi M_S \sim 8$ kOe) [25]. From our structural data we know that the cobalt phase for sample B is represented by the commonly oriented *hcp*-type cobalt structure. For the bulk *hcp*-Co phase the uniaxial anisotropy parameter is tabulated as well and is $H_K \approx 6$ kOe [25]. Taking into account the above-mentioned saturation magnetization of the bulk cobalt the $H_S \approx 12$ kOe for the *hcp*-Co thin film can be predicted. It states the clear discrepancy between the experimental and the estimated H_S values that points to the loss of the uniaxial magnetic out-of-plane anisotropy in the investigated *hcp*-Co phase of sample B. This fact indirectly correlates with the presence of uniaxial stacking faults (*rcp*-structure) within the *hcp*-cobalt extracted from our asymmetric XRD analysis.

Our magnetic and structural results as well as data reported for other Co/C systems prepared using DC-sputtering are summarized in Table 1. Here, one can see a clear trend where amorphous state of Co phase and the absence of carbide compounds are the main prerequisites for high saturation fields and simultaneously vanishing coercive fields.

5 Conclusions We study the C(5 nm)/Co/C(5 nm) multilayer stacks with cobalt thickness of 4 and 13 nm. Correspondingly for C/Co(4 nm)/C and C/Co(13 nm)/C samples, structural data reveal the presence of cobalt in the amorphous state and in the *hcp*-state with [0001] texture along the film surface normal. For both studied systems magnetic and structural data are in good agreement. For the 4-nm thick cobalt film our magnetic data show that cobalt amorphization (provided by the incorporation of carbon atoms in the growing cobalt layer) does not lead to the formation of carbides. We also show that strong inplane anisotropy can be introduced or eliminated in the amorphous cobalt film by controlling the parameters of DC-sputtering process. Compared to other sputtered Co/C thin-film systems our results – high saturation field of 1.6×10^4 Oe and vanishing inplane coercive field for C/Co/C multilayer stack with amorphous carbide-free cobalt film fit well into the overall trend. For the thicker *hcp*-type cobalt film we also deduce the presence of randomly close-packed structure. This type of *hcp* structure we assume to be responsible for the observed elimination of the out-of-plane magnetic anisotropy that is characteristic of *hcp*-cobalt phase.

References

[1] J. M. Slaughter and C. M. Falco, Nucl. Instrum. Methods Phys. Res. A **319**, 163–169 (1992).
[2] I. Artyukov, Ye. Bugayev, O. Devizenko, E. Gullikson, V. Kondratenko, and A. Vinogradov, Opt. Lett. **34**, 2930–2932 (2009).
[3] J. D. Jarratt and J. A. Barnard, IEEE Trans. Magn. **31**, 3952–3954 (1995).
[4] M. A. Rosa, M. Diego, E. Alves, N. P. Barradas, M. Godinho, M. Almeida, and A. P. Gonçalves, Phys. Status Solidi A **196**, 153–1156 (2003).
[5] S. M. Feng, G. L. Zhu, J. D. Shao, K. Yi, Z. X. Fan, and X. M. Dou, Appl. Phys. A **74**, 553–555 (2002).
[6] Q. Xue, W. Yang, A. Wei, and S. Hu, J. Magn. Magn. Mater. **46**, 379–381 (2002).
[7] M. Gabureac, L. Bernau, I. Utke, and G. Boero, Nanotechnology **21**, 115503 (2010).
[8] C. D. Stanciu, F. Hansteen, A. V. Kimel, A. Kirilyuk, A. Tsukamoto, A. Itoh, and Th. Rasing. Phys. Rev. Lett. **99**, 047601 (2007).
[9] M. Yu, Y. Liu, and D. J. Sellmyer, J. Appl. Phys. **85**, 4319–4321 (1999).
[10] R. Krishnan, H. O. Gupta, C. Sella, and M. Kaabouchi, J. Magn. Magn. Mater. **93**, 174–178 (1991).
[11] J. Shi, M. Azumi, and O. Nittono, Appl. Phys. A: Mater. Sci. Process. **73**, 215–218 (2000).
[12] H. Y. Sun, S. Z. Feng, X. F. Nie, and Y. P. Sun, J. Magn. Magn. Mater. **299**, 70–74 (2005).
[13] J. Delaunay, T. Haeashi, V. Tomita, and S. Hirono, J. Appl. Phys. **82**, 2200 (1997).

[14] S. Martens, O. Albrecht, K. Nielsch, and D. Görlitz, J. Appl. Phys. **105**, 07C113 (2009).
[15] I. A. Artyukov, V. V. Vinogradov, Ye. A. Bugayev, A. Yu. Devizenko, V. V. Kondratenko, and Yu. S. Kasyanov, J. Exp. Theor. Phys. **109**, 1009–1022 (2009).
[16] Ye. Bugaev, A. Devizenko, E. Zubarev, V. Sevrjukova, and V. Kondratenko, Metallofiz. Novejshie Tekhnol. **30**, 1533–1545 (2008).
[17] C. Casiraghi, A. C. Ferrari, J. Robertson, R. Ohr, M. Gradowski, D. Schneider, and H. Hilgers, Diamond Relat. Mater. **13**, 1480–1485 (2004).
[18] I. A. Artyukov, R. M. Feschenko, A. V. Vinogradov, Ye. A. Bugayev, O. Y. Devizenko, V. V. Kondratenko, Yu. S. Kasyanov, T. Hatano, M. Yamamoto, and S. V. Saveliev, Micron **41**, 722–728 (2010).
[19] T. Konno and R. Sinclar, Acta Met. Mater. **42**, 1231–1247 (1994).
[20] J. W. Feng, S. S. Kang, F. M. Pan, G. J. Jin, M. Lu, A. Hu, S. S. Jiang, and D. Feng, J. Magn. Magn. Mater. **152**, 27–27-32 (1996).
[21] H. Kockar, J. Supercond. **17**, 531–536 (2004).
[22] S. Yulin, T. Feigl, T. Kuhlmann, N. Kaiser, A. I. Fedorenko, V. V. Kondratenko, O. V. Poltseva, V. A. Sevryukova, A. Zolotaryov, and E. N. Zubarev, J. Appl. Phys. **92**, 1216–1220 (2002).
[23] I. Artyukov, Ye. Bugayev, O. Devizenko, R. Feschenko, Yu. Kasyanov, V. Kondratenko, S. Romanova, S. Saveliev, F. Schafers, Feiglf, Yu. Uspenski, and A. Vinogradov, Proc. SPIE **5919**, 59190E (2005).
[24] R. S. Iskhakov, S. V. Stolyar, L. A. Chekanova, E. M. Artem'ev, and V. S. Zhigalov, JETP Lett. **72**, 316–319 (2000).
[25] K. H. J. Buschow, Concise Encyclopedia of Magnetic and Superconducting Materials, 2nd ed. (Elsevier Ltd., Oxford, UK, 2005).
[26] H. Wang, S. P. Wong, W. Y. Cheung, N. Ke, W. F. Lau, M. F. Chiah, and X. X. Zhang, Mater. Sci. Eng., C **16**, 147–151 (2001).

